Adults vs. neonates: Differentiation of functional connectivity between the basolateral amygdala and occipitotemporal cortex

Heather A. Hansen[1*], Jin Li[1], and Zeynep M. Saygin[*]

[1]Department of Psychology, The Ohio State University, Columbus, Ohio, United States of America

* Corresponding authors

E-mails: hansen.508@osu.edu (HAH), saygin.3@osu.edu (ZMS)

Abstract

The amygdala, a subcortical structure known for social and emotional processing, consists of multiple subnuclei with unique functions and connectivity patterns. Tracer studies in adult macaques have shown that the basolateral subnuclei differentially connect to parts of visual cortex, with stronger connections to anterior regions and weaker connections to posterior regions; infant macaques show robust connectivity even with posterior visual regions. Do these developmental differences also exist in the human amygdala, and are there specific functional regions that undergo the most pronounced developmental changes in their connections with the amygdala? To address these questions, we explored the functional connectivity (from resting-state fMRI data) of the basolateral amygdala to occipitotemporal cortex in human neonates scanned within one week of life and compared the connectivity patterns to those observed in young adults. Specifically, we calculated amygdala connectivity to anterior-posterior gradients of the anatomically-defined occipitotemporal cortex, and also to putative occipitotemporal functional parcels, including primary and high-level visual and auditory cortices (V1, A1, face, scene, object, body, high-level auditory regions). Results showed a decreasing gradient of functional connectivity to the occipitotemporal cortex in adults – similar to the gradient seen in macaque tracer studies – but no such gradient was observed in neonates. Further, adults had stronger connections to high-level functional regions associated with face, body, and object processing, and weaker connections to primary sensory regions (i.e., A1, V1), whereas neonates showed the same amount of connectivity to primary and high-level sensory regions. Overall, these results show that functional connectivity between the amygdala and occipitotemporal cortex is not yet differentiated in neonates, suggesting a role of maturation and experience in shaping these connections later in life.

Introduction

How does emotional valence influence visual perception? Whether it be driving by an emotionally salient car crash or happening upon an animal carcass in the jungle, perceiving visual stimuli through an emotional lens can be critical for quick motor responses and ultimate survival. Emotionally salient cues preceding a target can enhance target perception (e.g., (1)), and perceiving aversive stimuli enhances blood flow to cortical regions (e.g., the middle temporal gyrus (2)). Developmentally, not only does visual acuity improve with age (3), but visual perceptual mechanisms of emotional stimuli are also fine-tuned with experience (e.g., (4)).

Emotional valence is canonically tied to the amygdala, an evolutionarily preserved neural structure known for emotional processing and regulation (e.g., (5,6)). The amygdala has been additionally implicated in social cognition and attention (e.g., (7)), fear recognition and conditioning (e.g., (8,9)), stimulus-value learning and reward (e.g., (10,11)), and novelty detection (e.g., (12,13)). The functions of the amygdala and the way in which the amygdala assigns valence to stimuli change across development (14). Similarly, visual perceptual skills and their neural correlates also change across development (15). Perceiving the identity of visual stimuli is commonly attributed to the occipitotemporal cortex, the location of the ventral visual stream and "what" pathway (e.g., (16)). It is posited that emotionally enhanced visual perception may occur via cortical feedback connections between the amygdala and visual cortex (17).

Work in macaques shows that projections from the amygdala subnuclei to the ventral visual stream are topographically organized on a gradient, such that visual cortical areas that are more rostral receive heavier amygdalar projections than visual cortical areas that are more caudal (18,19). Amaral and colleagues (19–22) found the basal subnucleus of the amygdala to especially follow this pattern, but noted additional projections from area TE to the lateral

subnucleus that creates a feedforward/feedback loop. Other work in adult macaques has similarly shown projections from areas TEO and TE to the lateral nucleus of the amygdala, and from area TE to the basal nucleus (23).

Interestingly, these connections change over development. Experiments comparing adult to juvenile animals, specifically in nonhuman primates (e.g., (23–26)) and rats (e.g., (27,28)), reveal that amygdalar projections are adult-like in juveniles, but that juveniles also have additional connections that are either totally eliminated with maturation or become more refined in their distribution.

Do these connections show a similar pattern in human development? We know that macaque cortex is oriented differently than human cortex, and although homologies exist, the connectivity pattern in macaques may not necessarily perfectly map to humans (29,30). Moreover, in humans, it is more challenging to study amygdalar connections at such a fine-grained level that tracer studies can provide, especially with respect to the basal vs. lateral nucleus and their connections to visual cortex. Several groups have used a variety of methods to parcellate the amygdala into two to four subunits (e.g., (31–37)). More recent work has made it possible to use local intensity differences in a typical T1 scan to divide the human amygdala into nine separate subunits (38), thus allowing a way to parcellate the amygdala using a standard resolution anatomical (T1) image and explore the connectivity of these subunits with a separate (independent) connectivity scan.

There is some previous work in humans that explores the developmental changes of amygdalar connectivity. A study that explored a cross-sectional sample of 5-30 year olds showed that DWI connectivity of the lateral and basal nuclei to cortical areas becomes increasingly sparse and localized with age (39). A functional connectivity study in 7-9 year olds vs. adults

found that the basolateral amygdala had stronger connectivity with temporal regions than the centromedial amygdala, and that overall connectivity was stronger in adults compared to children (34). Another study showed that basolateral functional connectivity to regions including parahippocampal gyrus, superior temporal cortex, and occipital lobe decreases with age across 4-23-year-olds (36), but that the basolateral amygdala showed increasing functional connectivity to occipital cortex between ages 3 months to 5 years (37). This last study is the opposite pattern than what was found in macaque development (i.e., decreasing connectivity to occipital cortex across age, e.g., (23)), and may be due to the differences between functional vs. white-matter connectivity or due to differences between macaques and humans. Moreover, it remains unclear why these connections change with development; the occipitotemporal cortex contains a multitude of well-studied visual and auditory functional areas. It is possible that amygdala connectivity changes with respect to functionally specific parts of occipitotemporal cortex that show increasing developmental specialization. To date, no study has investigated neonatal functional connectivity of the amygdala subnuclei and no study has investigated this connectivity with respect to putative functionally-distinct regions within visual and auditory cortex.

Does the rostrocaudal gradient of connectivity from the basolateral subnucleus observed in macaques match that of humans, or will a different pattern emerge? Does this connectivity pattern exist from birth, or develop later in life? And are the developmental changes in connectivity specific to certain functional parcels located within the occipitotemporal cortex? Here we investigate the developmental changes in functional connectivity between the basolateral amygdala and the occipitotemporal cortex using a cross-sectional sample of adults and neonates. In the first set of analyses we target the entire occipitotemporal cortex to recreate the connectivity work done in macaques. Then, we apply a unique approach by targeting

functionally defined regions in the ventral visual stream in order to draw conclusions about what might be driving the observed pattern of connectivity.

Method

Participants

Neonates

Forty neonates (15 female, mean gestational age at birth = 38.99 weeks, gestational age range at scan = 37-44 weeks) were obtained from the initial release of the Developing Human Connectome Project (dHCP, http://www.developingconnectome.org) (40). Neonates were scanned at the Evelina Neonatal Imaging Center in London, and the study was approved by the UK Health Research Authority.

Adults

Forty adults (15 female, age range 22-36 years) were obtained from the Human Connectome Project (HCP), WU-Minn HCP 1200 Subjects Data Release (https://www.humanconnectome.org/study/hcp-young-adult) (41). All participants were scanned at Washington University in St. Louis, MO. The forty adults used in this study were chosen to best motion- and sex-match the neonate sample: for each neonate, an adult from the HCP dataset with the same sex and most similar motion parameter (i.e., framewise displacement, FD) was determined using k-nearest neighbors. By using this approach, head motion in the final samples was not significantly different between groups ($t(78) = 0.77$, $p = 0.45$).

Acquisition and Preprocessing

Neonates

Images were acquired on a Philips 3T Achieva scanner using a specially designed neonatal 32 channel phased array head coil with dedicated slim immobilization pieces to reduce gross motion (42). All neonates (i.e., both MRI and fMRI scans) were scanned while in natural sleep. High-resolution (0.8 mm^3) structural scans were acquired on all participants. T2-weighted and inversion recovery T1-weighted multi-slice fast spin-echo images were acquired with in-plane resolution 0.8 x 0.8 mm^2 and 1.6 mm slices overlapped by 0.8 mm (T2-weighted: TE/TR = 156/12000ms; T1 weighted: TE/TR/TI = 8.7/4795/1740ms). Structural MRI data were preprocessed in FreeSurfer v.6.0.0 (http://surfer.nmr.mgh.harvard.edu/fswiki/infantFS) using a dedicated infant processing pipeline (40,43,44) which includes motion and intensity correction, surface coregistration, spatial smoothing, subcortical segmentation, and cortical parcellation based on spherical template registration; FreeSurfer was used for amygdala segmentation (38). Gray and white matter masks were obtained from segmentations of the T2w volume using the DRAW-EM algorithm provided by dHCP (45). The resulting cortical and subcortical segmentations were reviewed for quality control.

Resting-state fMRI data were also acquired on all participants, using multiband (MB) 9x accelerated echo-planar imaging (TE/TR = 38/392ms, voxel size = 2.15 mm^3) developed for neonates (see (46) for details). The resting-state scan lasted approximately 15 min and consisted of 2300 volumes for each run. No in-plane acceleration or partial Fourier was used. Single-band reference scans were also acquired with bandwidth-matched readout, as well as additional spin-echo acquisitions with both AP/PA fold-over encoding directions. The data released by the dHCP included minimal preprocessing of the resting-state fMRI data (see (46)) which included distortion-correction, motion-correction, 2-stage registration of the MB-EPI functional image to the T2 structural image, generation of a combined transform from MB-EPI to the 40-week T2

template, temporal high-pass filtering (150 s high-pass cutoff), and independent component analysis (ICA) denoising using FSL FIX. Additional preprocessing included smoothing within gray matter (Gaussian filter with FWHM = 3 mm), and a band-pass filter at 0.009-0.08 Hz. To further denoise, aCompCor (47) was used to regress out signals from white matter and cerebrospinal fluid (CSF) which controls physiological noise (e.g., respiration, heartbeat) and non-neural contributions to the resting state signal. All functional connectivity analyses for the neonatal group were performed in native functional space.

Adults

Images were acquired on a customized 3T Connectome Scanner adapted from a Siemens Skyra (Siemens AG, Erlanger, Germany). The 32-channel scanner had a receiver head coil and a body transmission coil specifically designed by Siemens for the WU-Minn and MGH-UCLA Connectome scanners.

High-resolution T2-weighted and T1-weighted structural scans were acquired on all participants. Images were acquired with 0.7 mm^3 isotropic voxel resolution (T2-weighted 3D T2-SPACE scan: TE/TR = 565/3200ms; T1-weighted 3D MPRAGE: TE/TR/TI = 2.14/2400/1000ms). The data that were released had undergone preprocessing using the HCP minimal preprocessing pipelines (see (48) for details), which included: gradient distortion correction, ACPC registration to produce an undistorted “native” structural volume space, brain extraction, bias field correction, and registration from the T2-weighted scan to the T1-weighted scan. Each adult brain was aligned to a common MNI152 template with 0.7 mm isotropic resolution. Then, a FreeSurfer pipeline (based on FreeSurfer 5.3.0-HCP) specifically designed for HCP data was used to segment the volume into predefined structures, reconstruct white and

pial cortical surfaces, and perform folding-based surface registration to their surface atlas (fsaverage).

Resting-state fMRI data were also acquired on all participants, using the gradient-echo EPI sequence (TE/TR = 33.1/720ms, flip angle = 52°, number of slices = 72, voxel size = 2 × 2 × 2 mm^3). The resting-state scan lasted approximately 15 min and consisted of 1200 volumes for each run. All participants completed two resting-state fMRI sessions, each consisting of one run with two phases encoding in a right-to-left (RL) direction and one run with phase encoding in a left-to-right (LR) direction; the current analysis uses the LR phase encoding from the first session. Participants were instructed to open their eyes with relaxed fixation on a projected bright cross-hair on a dark background. The data that were released had undergone minimal preprocessing (48), which included removal of spatial distortions, motion correction, registration of the fMRI data to both the structural and MNI-152 template, bias field reduction, and denoising using the novel ICA-FIX method. In order to preprocess these data in a pipeline that mirrored the neonatal group, we unwarped the data from MNI-152 to native space, then applied spatial smoothing (Gaussian filter with FWHM = 3 mm) within all gray matter, band-pass filtered at 0.009-0.08 Hz, and implemented aCompCor (47).

Defining regions of interest

Amygdala subnuclei

Using automated segmentation (38), nine amygdala subnuclei (lateral, basal, accessory basal, central, medial, cortical, paralaminar, cortico-amygdaloid transition area, anterior amygdala area) were parcellated in each individual's native anatomical space and then transferred to functional space. Because the lateral and basal subnuclei are associated with sensory and cognitive processes (49,50) and thus likely contribute to emotional visual perception, the combined

basolateral subnucleus was the main seed of interest in the present experiment. Fig S1 compares the basolateral amygdala segmentation in neonates with the dHCP-provided amygdala labels; we found that almost all of the basolateral amygdala used here was within the dHCP manually-labeled amygdala (proportion of BaLa within dHCP amygdala: 0.76 ± 0.11).

Occipitotemporal cortex

Anatomical divisions. To explore the connectivity of the basolateral amygdala to occipitotemporal cortex (OTC), an OTC label was made for each individual using anatomical labeling provided by each data set (i.e., DRAW-EM labels for neonates, aparc+aseg labels for adults; see Supplement for labels used and Fig S2 for a depiction of labels in a neonate vs. adult) that combined all anatomical regions in the occipital and temporal cortices. The OTC label was transferred from native anatomical space to functional space for each subject. In order to track differences in connectivity across the region, the label was split (separately for each individual and each hemisphere) into five equal sections from anterior to posterior. These five anatomical OTC sections were the connectivity targets for the first analyses (see Fig 1A).

Functional parcels. To explore the functional significance of connectivity patterns, functional parcels that encompass primary and secondary visual and auditory areas within the OTC were identified. All parcels that we used are available online and/or by contacting the corresponding author of the cited publications. The parcels were originally created via the group-constrained subject-specific method (GSS) (51), which generates probabilistic maps of functional activation across independent groups of participants and creates parcels that encapsulate most individuals' functional regions. We used the face-selective fusiform face area (FFA), occipital face area (OFA), and superior temporal sulcus (STS); object-selective lateral occipital cortex (LO) and posterior fusiform sulcus (PFS); scene-selective parahippocampal

place area (PPA) and retrosplenial cortex (RSC) from (52); and high-level auditory region superior temporal gyrus (STG), a region in vicinity of primary auditory cortex involved in speech perception (53). In addition, primary visual cortex (V1) and auditory cortex (A1) were anatomically defined in each subject using the calcarine sulcus and Heschl's gyrus from FreeSurfer Desikan parcellation (54), respectively. See Fig 2A for an illustration of the parcels.

Functional parcels were mapped to the FreeSurfer CVS average-35 in MNI152 brain (if not already publicly provided in that space) and were subsequently overlaid onto each individual's anatomical brain using Advanced Normalization Tools (ANTs version 2.1.0; http://stnava.github.io/ANTs) (55). The parcels were then converted to native functional space using nearest neighbor interpolation with FreeSurfer's mri_vol2vol function (https://surfer.nmr.mgh.harvard.edu/fswiki/mri_vol2vol). For any parcels that overlapped, intersecting voxels were assigned to the functional parcel with smaller size; this ensured that no voxel belonged to more than one functional parcel, and additionally compensated for size differences. Finally, voxels within white matter and cerebellum were removed.

Functional connectivity analyses

The mean time course of the basolateral amygdala, each OTC section, and each functional parcel was computed from the preprocessed resting state images. Functional connectivity (FC) was calculated using Pearson's correlations between the time courses of the basolateral seed and each target region, collapsed across hemispheres. To generate normally distributed values, each FC value was Fisher z-transformed.

Connectivity differences were calculated using 2-way mixed ANOVAs, with sample (adults vs. neonates) as the between-subject variable and target (i.e., different anatomical/functional regions of interest) as the within-subject variable. Paired *t*-tests were

conducted for within-group comparisons and independent *t*-tests for between-group comparisons. The Holm-Bonferroni method was used to correct for multiple comparisons for each post-hoc test; corrected *p*-values are denoted as p_{HB}.

Finally, we created FC fingerprint plots to elucidate between-group differences. For each set of targets, connectivity values were mean-centered across subjects in each sample by subtracting the mean FC across all targets from the mean FC of each individual target. Thus, the fingerprint plots indicate how the basolateral amygdala connects to the targets in each sample, accounting for average differences in connectivity.

Results

Anatomically defined OTC

A 2 (sample) x 5 (OTC section) ANOVA was conducted to assess how basolateral amygdala connectivity to the occipitotemporal cortex changes across development. There was a significant main effect of sample, $F(1,390) = 22.42$, $p = 3.08 \times 10^{-6}$, and OTC section, $F(4,390) = 20.97$, $p = 1.13 \times 10^{-15}$. More specifically, across samples, connectivity to each of the sections decreased on a gradient from anterior to posterior, with significantly more connectivity to OTC 5 than OTC 4 ($t(79) = -4.44$, $p_{HB} = 1.45 \times 10^{-4}$), to OTC 4 than OTC 3 ($t(79) = -2.55$, $p_{HB} = 0.03$), to OTC 3 than OTC 2 ($t(79) = -4.04$, $p_{HB} = 5.01 \times 10^{-4}$), and to OTC 2 than OTC 1 ($t(79) = -2.06$, $p_{HB} = 0.04$). See Table S1 for all OTC statistical comparisons.

Importantly, the sample x OTC interaction was also significant, $F(4,390) = 13.22$, $p = 4.15 \times 10^{-10}$. To probe this interaction post hoc, a one-way ANOVA was conducted separately for each sample across the OTC sections (Fig 1B). Whereas the adult sample showed a significant main effect of OTC section ($F(4,195) = 28.76$, $p = 8.63 \times 10^{-19}$), the neonate sample did not

$F(4,195) = 2.05$, $p = 0.09$). Adults showed decreasing connectivity on a gradient from OTC 5 to OTC 4 ($t(39) = -2.91$, $p_{HB} = 0.01$), OTC 4 to OTC 3 ($t(39) = -1.99$, $p_{HB} = 0.05$), OTC 3 to OTC 2 ($t(39) = -6.06$, $p_{HB} = 2.60 \times 10^{-6}$), and OTC 2 to OTC 1 ($t(39) = -3.53$, $p_{HB} = 3.20 \times 10^{-3}$). Although a main effect of OTC section was not observed in neonates, planned t-tests were run to quantify a gradient: neonates showed differentiation between OTC 5 and OTC 4 ($t(39) = -3.33$, $p_{HB} = 0.02$), but connectivity to the rest of the subsequent OTC sections was not significantly different. The differential patterns of connectivity between adults and neonates is additionally represented in an FC fingerprint plot (Fig 1C); the mean-centered connectivity within all five OTC sections significantly differed between adults and neonates. See Table S2 and Table S3 for all within- and between-sample OTC statistical comparisons, respectively.

Fig 1. Anatomical Regions and Functional Connectivity Results. (A) Basolateral (BaLa) amygdala and anatomical targets used for connectivity analyses. Left, an example parcellation of the basal and lateral amygdala subnuclei in a representative subject, using the atlas developed by Saygin et al., 2017. Right, depiction of the 5 occipitotemporal cortex (OTC) labels in a representative subject. Labels marked from most anterior (OTC 5, dark blue) to most posterior (OTC 1, dark green). (B) Bar plot of mean functional connectivity to each of the 5 OTC sections arranged from anterior to posterior for each sample, with adults in gray and neonates in red. Error bars are standard error of the mean. †$p<0.06$, *$p<0.05$, *$p<0.01$, ***$p<0.001$ (C) FC fingerprint plot depicting the pattern of connectivity of both samples. Axes are mean centered FC values for each sample.

Functionally defined regions within OTC

Parcels

A 2 (sample) x 11 (functional parcel) ANOVA was conducted to assess how basolateral amygdala connectivity to functional parcels within the occipitotemporal cortex changes across

development. Again, there was a significant main effect of sample, $F(1,858) = 19.43$, $p = 1.18 \times 10^{-5}$, and parcel, $F(10,858) = 6.39$, $p = 1.57 \times 10^{-9}$.

Additionally, the sample x parcel interaction was also significant, $F(10,858) = 10.43$, $p = 9.21 \times 10^{-17}$. To probe this interaction post hoc, a one-way ANOVA was conducted separately for each sample across the 11 parcels (Fig 2B). Again, whereas the adult sample showed a significant main effect of functional parcel ($F(10,429) = 13.77$, $p = 4.04 \times 10^{-21}$), the neonate sample did not $F(10,429) = 0.78$, $p = 0.65$). Post-hoc t-tests were only conducted on adults (see Table S4 for all comparisons in adults); of particular note, adults showed significantly different connectivity between parcels within the same OTC section, such as A1 and STG within OTC 4 ($t(39) = -5.68$, $p_{HB} = 8.14 \times 10^{-5}$), and between OFA and V1 within OTC 1 ($t(39) = 6.08$, $p_{H\,B} = 2.35 \times 10^{-5}$), whereas neonates did not show an effect of functional parcel.

Fig 2. Functional Parcels and Functional Connectivity Results. (A) Basolateral (BaLa) amygdala and functional targets used for connectivity analyses. Left, BaLa parcellation in a representative subject. Right, depiction of the 11 functional parcels used as targets. (B) Bar plot of mean functional connectivity to each of the 11 parcels arranged from anterior to posterior for each sample, with adults in gray and neonates in red. X-axis color represents OTC section where majority of parcel is located, from blue (OTC 4, A1 and STG) to dark green (OTC 1, OFA and V1). Error bars are standard error of the mean. Significance depicted between regions within the same OTC section only. *p<0.05, **p<0.01, ***p<0.001

Categories

To probe whether the connectivity differences across the parcels could better be attributed to overall function rather than anatomical location, a 2 (sample) x 7 (functional category) ANOVA was conducted to assess how basolateral amygdala connectivity to functional categories changes across development. As before, there was a significant main effect of sample, $F(1,546) = 7.19$, $p = 0.01$, and category, $F(6,546) = 9.02$, $p = 2.08 \times 10^{-9}$.

Additionally, the sample x category interaction was also significant, $F(6,546) = 14.97$, $p = 6.96 \times 10^{-16}$. To probe this interaction post hoc, a one-way ANOVA was conducted separately for each sample across the 7 categories (Fig 3A). Again, whereas the adult sample showed a significant main effect of functional category ($F(6,273) = 20.42$, $p = 9.90 \times 10^{-20}$), the neonate sample did not $F(6,273) = 0.62$, $p = 0.71$). As depicted in Fig 3A, adults showed more connectivity to parcels that functionally process faces, bodies, objects, and high-level auditory processing, and less connectivity to parcels that functionally process scenes and primary auditory and visual cortex. Neonates showed undifferentiated connectivity across categories. As indicated in the FC fingerprint plot (Fig 3B), all seven functional categories exhibited significant between-group differences in mean-centered connectivity patterns. See Table S5 and Table S6 for all statistical comparisons within adults and between samples, respectively.

Fig 3. Functional Connectivity to Functional Categories. (A) Bar plot of mean functional connectivity to each of the 7 functional categories, with adults in gray and neonates in red. Error bars are standard error of the mean. *p<0.05, **p<0.01, ***p<0.001 (C) FC fingerprint plot depicting the pattern of connectivity of both samples. Axes are mean centered FC values for each sample. Parentheses show which of the 11 parcels were included in each category. Asterisks denote significance between groups for each category.

Discussion

Investigating the functional connectivity between the amygdala and occipitotemporal cortex will help us better understand the amygdala's role in perceiving and processing emotional visual stimuli, which has ecological relevance and certainly changes across development. Many functionally specialized visual regions exist within occipitotemporal cortex, but it was previously unknown how connectivity to these regions develops from birth in humans. Previous work in

345 macaques had revealed connections between the lateral and basal amygdala subnuclei and the
346 occipitotemporal cortex, noting a rostrocaudal topographic organization of the connections (e.g.,
347 (22)) and refinement across development (e.g., (23)). In this paper, we explored this topographic
348 organization in humans using functional connectivity, and further investigated specific functional
349 cortical areas located within the occipitotemporal region that may contribute to the observed
350 pattern of connectivity.

351 In our study, connectivity between the basolateral amygdala and occipitotemporal cortex
352 in human adults decreased on a gradient from anterior to posterior, replicating the finding in
353 macaques. However, the connectivity in neonates was largely undifferentiated, suggesting that
354 the topographic organization in adulthood is not yet present at birth. Splitting the cortex into
355 functionally defined parcels allowed us to further hone in on the developmental changes in this
356 pattern. If the gradient of connectivity was reliant on anatomical location (e.g., cortex closer to
357 the amygdala is more functionally connected), then splitting the cortex into parcels should have
358 revealed a comparable gradient. Instead, the parcels had varied connectivity with the amygdala
359 in adults, even when anatomically located in the same OTC section. For instance, within more
360 anterior regions of the OTC, connectivity was driven more by connections with STG (known for
361 processing high-level auditory information, e.g., speech) than with adjacent A1 (primary
362 auditory cortex). Similarly, in posterior OTC, lower connectivity in adults was driven more by
363 connections with V1 (primary visual cortex) than by connections with OFA (known for
364 processing faces). This would suggest that functional processing of the cortex contributes to the
365 development of connectivity between the amygdala and OTC: adults showed more connectivity
366 to high-level sensory regions (i.e., regions processing faces, bodies, objects, high-level audition)
367 relative to primary sensory regions (i.e., V1, A1). Conversely, neonates had similar connectivity

to all functional parcels and categories, with not much differentiation among them. Interestingly, V1 showed the largest developmental difference between the two samples, with positive connectivity in neonates and negative connectivity in adults. These results are in line with studies in macaques (e.g., (23,24)) where both adult and infant macaques showed comparably high amygdalar connectivity with anterior temporal cortex, but only infants showed additional connections to posterior OTC regions. Human neonates and adults in the present study also showed relatively high connectivity to anterior OTC, but only neonates showed high connectivity with posterior OTC.

The present study also revealed noticeable differences in amygdalar connectivity to each of the distinct functional categories in adults, where basolateral connectivity was highest with face, body, and high-level auditory regions. This pattern of differential connection strength was largely absent in neonates, who showed similar strength of connection to almost all of the functional regions. Previous work in infants found similarities in amygdalar functional circuitry in infants as in adults (37), as well as similar (but still immature) functional organization of visual cortex in infants as in adults (56). Although informative, these particular studies used samples of infants between the ages of 2.3-8.6 months; the present study examines neonates with gestational age between 37-44 weeks. Given that the neonates showed largely undifferentiated connectivity of the basolateral amygdala with various functional regions compared to adults, but functional organization appears more adult-like after a few months in other studies, we posit that adult-like connectivity between the basolateral amygdala and functional regions of the OTC are not present at birth and instead require at least some experience (i.e., a few months) to develop. This is in line with previous work suggesting that refinement and pruning of connections typically occur after relevant cognitive milestones and neural specialization occur (57–59).

Experience with the environment postnatally may lead to notable age-related changes, and activity-dependent interactions between cortical regions may fine-tune their functionality. The functional maturation of the occipitotemporal regions that were studied here may contribute to the continued refinement of the amygdalar subregions, the amygdalar connections to these regions, and to the functional specialization of occipitotemporal regions themselves (e.g. in line with Interactive Specialization theories of development; (60)).

One notable limitation of the present study is that we use functional parcels originally defined in adults, and recognize that overlaying them onto neonates may have the potential to overestimate or mischaracterize certain cortex. However, we used ANTs to register the functional parcels to each neonate's native space, which has been shown to be highly effective and reliable (61). These limitations can only be overcome by functionally defining regions of interest in each individual, which may not be reliable in a sample of newborns (see (62) for a review of neuroimaging methods in adults vs. neonates), or perhaps with longitudinal studies that can functionally localize regions using task-based fMRI at a later age and register them to the same individual's connectivity scan at an earlier age (e.g., (63)).

Overall, the present experiments make apparent a decreasing pattern of connectivity between the amygdala and posterior aspects of occipitotemporal cortex, evidence for which has been repeatedly shown in macaques but was otherwise lacking in humans. Further, we contrast adult data with a sample of neonates scanned within one week of birth, to gauge what connectivity exists primitively, prior to extensive experience with the world. Additionally, we identify putative functional areas in the ventral visual stream that might be driving the observed pattern of connectivity changes. This work has important clinical applications: Given the role of the amygdala in many psychiatric disorders – many of which have early onsets, such as autism

and anxiety (e.g., (35,64–67)) – it is crucial to fully understand how the amygdala connects to the rest of the brain across early development. The developmental progression of connectivity between the amygdala and occipitotemporal cortex in typically-developing humans can help us better understand developmental disorders or deficits implicated when these connections are abnormal or lacking. Further research can seek to explore this connectivity in patient populations, classify differences between patients and controls, and offer new diagnostic or treatment interventions.

Acknowledgements

Analyses were completed using the Ohio Supercomputer Cluster (https://www.osc.edu). We would like to thank the Human Connectome Project (https://www.humanconnectome.org) and developing Human Connectome Project (http://www.developingconnectome.org), David Osher for comments and suggestions, and members of Z-Lab (Saygin Developmental Cognitive Neuroscience Lab) for feedback and comments.

References

1. Phelps EA, Ling S, Carrasco M. Emotion facilitates perception and potentiates the perceptual benefits of attention. Psychol Sci. 2006;17(4):292–9.
2. Kosslyn SM, Shin LM, Thompson WL, McNally RJ, Rauch SL, Pitman RK, et al. Neural effects of visualizing and perceiving aversive stimuli (PET). Neuroreport. 1996;7(10):1569–76.
3. Teller DY, McDonald M, Preston K, Sebris SL, Dobson V. Assessment of visual acuity in infants and children: The acuity card procedure. Dev Med Child Neurol. 1986;28:779–89.
4. Leppänen JM, Nelson CA. Tuning the developing brain to social signals of emotions. Nat Rev Neurosci. 2009;10(1):37–47.
5. Ochsner KN, Silvers JA, Buhle JT. Functional imaging studies of emotion regulation: a synthetic review and evolving model of the cognitive control of emotion. Ann N Y Acad Sci. 2012;1251:1–24.
6. Phillips ML, Drevets WC, Rauch SL, Lane R. Neurobiology of Emotion Perception I: The Neural Basis of Normal Emotion Perception. Biol Psychiatry. 2003;54:504–14.
7. Adolphs R, Spezio M. Role of the amygdala in processing visual social stimuli. Prog Brain Res. 2006;156:363–78.
8. Adolphs R, Gosselin F, Buchanan TW, Tranel D, Schyns P, Damasio AR. A mechanism for impaired fear recognition after amygdala damage. Lett to Nat. 2005;433:68–72.
9. Phillips RG, Ledoux JE. Differential Contribution of Amygdala and Hippocampus to Cued and Contextual Fear Conditioning. Behav Neurosci. 1992;106(2):274–85.
10. Baxter MG, Murray EA. The amygdala and reward. Nat Rev Neurosci. 2002;3:563–73.
11. Paton JJ, Belova MA, Morrison SE, Salzman CD. The primate amygdala represents the

positive and negative value of visual stimuli during learning. Nature. 2006;439(February):865–70.

12. Kiehl KA, Stevens MC, Laurens KR, Pearlson G, Calhoun VD, Liddle PF. An adaptive reflexive processing model of neurocognitive function: supporting evidence from a large scale (n = 100) fMRI study of an auditory oddball task. Neuroimage. 2005;25:899–915.

13. Schwartz CE, Wright CI, Shin LM, Kagan J, Whalen PJ, Mcmullin KG, et al. Differential Amygdalar Response to Novel versus Newly Familiar Neutral Faces: A Functional MRI Probe Developed for Studying Inhibited Temperament. Biol Psychiatry. 2003;3223(53):854–62.

14. Tottenham N, Hare TA, Casey BJ. A developmental perspective on human amygdala function. In: The human amygdala. New York, NY, US: The Guilford Press; 2009. p. 107–17.

15. Atkinson J. The Developing Visual Brain [Internet]. Oxford Psychology Series. Oxford: Oxford University Press; 2002. 200 p. Available from: https://www.oxfordscholarship.com/10.1093/acprof:oso/9780198525998.001.0001/acprof-9780198525998

16. Goodale MA, Milner AD. Separate visual pathways for perception and action. Trends Neurosci. 1992;15(1):20–5.

17. Vuilleumier P. How brains beware: neural mechanisms of emotional attention. Trends Cogn Sci. 2005;9(12):585–94.

18. Iwai E, Yukie M, Suyama H, Shirakawa S. Amygdalar connections with middle and inferior temporal gyri of the monkey. Neurosci Lett. 1987;83(1–2):25–9.

19. Amaral DG, Price JL. Amygdalo-cortical projections in the monkey (Macaca fascicularis).

476 J Comp Neurol [Internet]. 1984 Dec 20;230(4):465–96. Available from:
477 https://doi.org/10.1002/cne.902300402
478 20. Amaral DG. The Primate Amygdala and the Neurobiology of Social Behavior:
479 Implications for Understanding Social Anxiety. Biol Psychiatry. 2002;51:11–7.
480 21. Amaral DG, Behniea H, Kelly JL. Topographic organization of projections from the
481 amygdala to the visual cortex in the macaque monkey. Neuroscience. 2003;118(4):1099–
482 120.
483 22. Freese JL, Amaral DG. Synaptic organization of projections from the amygdala to visual
484 cortical areas TE and V1 in the macaque monkey. J Comp Neurol. 2005;496(5):655–67.
485 23. Webster MJ, Ungerleider LG, Bachevalier J. Connections of Inferior Temporal Areas TE
486 and TEO with Medial Temporal-Lobe Structures in Infant and Adult Monkeys. J
487 Neurosci. 1991;11(4):1095–116.
488 24. Webster MJ, Ungerleider LG, Bachevalier J. Lesions of inferior temporal area TE in
489 infant monkeys alter cortico-amygdalar projections. Neuroreport. 1991;2:769–72.
490 25. Kalin NH, Shelton SE, Davidson RJ, Kelley AE. The Primate Amygdala Mediates Acute
491 Fear But Not the Behavioral and Physiological Components of Anxious Temperament. J
492 Neurosci. 2001;21(6):2067–74.
493 26. Kalin NH, Shelton SE, Takahashi LK. Defensive Behaviors in Infant Rhesus Monkeys :
494 Ontogeny and Context-Dependent Selective Expression. Child Dev. 1991;62(5):1175–83.
495 27. Bouwmeester H, Smits K, Ree JM Van. Neonatal Development of Projections to the
496 Basolateral Amygdala From Prefrontal and Thalamic Structures in Rat. J Comp Neurol.
497 2002;450:241–55.
498 28. Bouwmeester H, Wolterink G, Ree JMVR. Neonatal Development of Projections From

the Basolateral Amygdala to Prefrontal , Striatal , and Thalamic. J Comp Neurol. 2002;442:239–49.

29. Passingham R. How good is the macaque monkey model of the human brain? Curr Opin Neurobiol. 2009;19(1):6–11.

30. Van Essen DC, Donahue C, Dierker DL, Glasser MF. Parcellations and Connectivity Patterns in Human and Macaque Cerebral Cortex. 2016. 89–106 p.

31. Saygin ZM, Osher DE, Augustinack J, Fischl B, Gabrieli JDE. Connectivity-based segmentation of human amygdala nuclei using probabilistic tractography. Neuroimage [Internet]. 2011;56(3):1353–61. Available from: http://dx.doi.org/10.1016/j.neuroimage.2011.03.006

32. Bach DR, Behrens TE, Garrido L, Weiskopf N, Dolan RJ. Deep and Superficial Amygdala Nuclei Projections Revealed In Vivo by Probabilistic Tractography. J Neurosci [Internet]. 2011;31(2):618–23. Available from: http://www.jneurosci.org/cgi/doi/10.1523/JNEUROSCI.2744-10.2011

33. Brown VM, Labar KS, Haswell CC, Gold AL, Beall SK, Van Voorhees E, et al. Altered resting-state functional connectivity of basolateral and centromedial amygdala complexes in posttraumatic stress disorder. Neuropsychopharmacology [Internet]. 2014;39(2):351–9. Available from: http://dx.doi.org/10.1038/npp.2013.197

34. Qin S, Young CB, Supekar K, Uddin LQ, Menon V. Immature integration and segregation of emotion-related brain circuitry in young children. Proc Natl Acad Sci. 2012;109(20):7941–6.

35. Qin S, Young CB, Duan X, Chen T, Supekar K, Menon V. Amygdala subregional structure and intrinsic functional connectivity predicts individual differences in anxiety

during early childhood. Biol Psychiatry [Internet]. 2014;75(11):892–900. Available from: http://dx.doi.org/10.1016/j.biopsych.2013.10.006

36. Gabard-Durnam LJ, Flannery J, Goff B, Gee DG, Humphreys KL, Telzer E, et al. The development of human amygdala functional connectivity at rest from 4 to 23 years : A cross-sectional study. Neuroimage [Internet]. 2014;95:193–207. Available from: http://dx.doi.org/10.1016/j.neuroimage.2014.03.038

37. Gabard-Durnam LJ, O'Muircheartaigh J, Dirks H, Dean DC, Tottenham N, Deoni S. Human amygdala functional network development: A cross-sectional study from 3 months to 5 years of age. Dev Cogn Neurosci [Internet]. 2018;34(June):63–74. Available from: https://doi.org/10.1016/j.dcn.2018.06.004

38. Saygin ZM, Kliemann D, Iglesias JE, van der Kouwe AJW, Boyd E, Reuter M, et al. High-resolution magnetic resonance imaging reveals nuclei of the human amygdala: manual segmentation to automatic atlas. Neuroimage [Internet]. 2017;155(May):370–82. Available from: http://dx.doi.org/10.1016/j.neuroimage.2017.04.046

39. Saygin ZM, Osher DE, Koldewyn K, Martin RE, Finn A, Saxe R, et al. Structural connectivity of the developing human amygdala. PLoS One. 2015;10(4):1–19.

40. Makropoulos A, Robinson EC, Schuh A, Wright R, Fitzgibbon S, Bozek J, et al. The developing human connectome project: A minimal processing pipeline for neonatal cortical surface reconstruction. Neuroimage [Internet]. 2018;173:88–112. Available from: https://doi.org/10.1016/j.neuroimage.2018.01.054

41. Van Essen DC, Smith SM, Barch DM, Behrens TEJ, Yacoub E, Ugurbil K. The WU-Minn Human Connectome Project: An overview. Neuroimage [Internet]. 2013;80:62–79. Available from: http://www.sciencedirect.com/science/article/pii/S1053811913005351

545 42. Hughes EJ, Winchman T, Padormo F, Teixeira R, Wurie J, Sharma M, et al. A Dedicated
546 Neonatal Brain Imaging System. Magn Reson Med. 2017;78:794–804.
547 43. de Macedo Rodrigues K, Ben-Avi E, Sliva DD, Choe M, Drottar M, Wang R, et al. A
548 FreeSurfer-compliant consistent manual segmentation of infant brains spanning the 0 – 2
549 year age range. Front Hum Neurosci. 2015;9(February):1–12.
550 44. Zollei L, Ou Y, Iglesias J, Grant EP, Fischl B. FreeSurfer image processing pipeline for
551 infant clinical MRI images. In: Proceedings of the Organization for Human Brain
552 Mapping Conference. 2017.
553 45. Makropoulos A, Gousias IS, Ledig C, Aljabar P, Serag A, Hajnal J V, et al. Automatic
554 Whole Brain MRI Segmentation of the Developing Neonatal Brain. IEEE Trans Med
555 Imaging. 2014;33(9):1818–31.
556 46. Fitzgibbon SP, Harrison SJ, Jenkinson M, Baxter L, Robinson EC, Bastiani M, et al. The
557 developing Human Connectome Project (dHCP) automated resting-state functional
558 processing framework for newborn infants. bioRxiv [Internet]. 2019 Jan 1;766030.
559 Available from: http://biorxiv.org/content/early/2019/09/12/766030.abstract
560 47. Salimi-Khorshidi G, Douaud G, Beckmann CF, Glasser MF, Griffanti L, Smith SM.
561 Automatic denoising of functional MRI data: Combining independent component analysis
562 and hierarchical fusion of classifiers. Neuroimage [Internet]. 2014;90:449–68. Available
563 from: http://www.sciencedirect.com/science/article/pii/S1053811913011956
564 48. Glasser MF, Sotiropoulos SN, Wilson JA, Coalson TS, Fischl B, Andersson JL, et al. The
565 minimal preprocessing pipelines for the Human Connectome Project. Neuroimage
566 [Internet]. 2013;80:105–24. Available from:
567 http://www.sciencedirect.com/science/article/pii/S1053811913005053

568 49. Johansen JP, Hamanaka H, Monfils MH, Behnia R, Deisseroth K, Blair HT, et al. Optical
569 activation of lateral amygdala pyramidal cells instructs associative fear learning. Proc Natl
570 Acad Sci [Internet]. 2010;107(28):12692–7. Available from:
571 http://www.pnas.org/lookup/doi/10.1073/pnas.1002418107
572 50. Stefanacci L, Amaral DG. Some Observations on Cortical Inputs to the Macaque Monkey
573 Amygdala: An Anterograde Tracing Study. J Comp Neurol. 2002;451(May):301–23.
574 51. Fedorenko E, Hsieh P-J, Nieto-Castañón A, Whitfield-Gabrieli S, Kanwisher N. New
575 Method for fMRI Investigations of Language: Defining ROIs Functionally in Individual
576 Subjects. J Neurophysiol [Internet]. 2010 Apr 21;104(2):1177–94. Available from:
577 https://doi.org/10.1152/jn.00032.2010
578 52. Julian JB, Fedorenko E, Webster J, Kanwisher N. An algorithmic method for functionally
579 defining regions of interest in the ventral visual pathway. Neuroimage [Internet].
580 2012;60(4):2357–64. Available from: http://dx.doi.org/10.1016/j.neuroimage.2012.02.055
581 53. Basilakos A, Smith KG, Fillmore P, Fridriksson J, Fedorenko E. Functional
582 Characterization of the Human Speech Articulation Network. Cereb Cortex [Internet].
583 2018 Apr 27;28(5):1816–30. Available from: https://doi.org/10.1093/cercor/bhx100
584 54. Desikan RS, Ségonne F, Fischl B, Quinn BT, Dickerson BC, Blacker D, et al. An
585 automated labeling system for subdividing the human cerebral cortex on MRI scans into
586 gyral based regions of interest. Neuroimage. 2006;31(3):968–80.
587 55. Avants BB, Tustison NJ, Song G, Cook PA, Klein A, Gee JC. A reproducible evaluation
588 of ANTs similarity metric performance in brain image registration. Neuroimage [Internet].
589 2011;54(3):2033–44. Available from: http://dx.doi.org/10.1016/j.neuroimage.2010.09.025
590 56. Deen B, Richardson H, Dilks DD, Takahashi A, Keil B, Wald LL, et al. Organization of

high-level visual cortex in human infants. Nat Commun [Internet]. 2017 Jan 10;8:13995. Available from: http://dx.doi.org/10.1038/ncomms13995

57. Gogtay N, Giedd JN, Lusk L, Hayashi KM, Greenstein D, Vaituzis AC, et al. Dynamic mapping of human cortical development during childhood through early adulthood. Proc Natl Acad Sci. 2004;101(21):8174–9.

58. O'Leary DDM. Development of connectional diversity and specificity in the mammalian brain by the pruning of collateral projections. Curr Opin Neurobiol. 1992;2:70–7.

59. Khundrakpam BS, Reid A, Brauer J, Carbonell F, Lewis J, Ameis S, et al. Developmental Changes in Organization of Structural Brain Networks. Cereb Cortex. 2013;23:2072–85.

60. Johnson MH. Interactive Specialization: A domain-general framework for human functional brain development? Dev Cogn Neurosci. 2010;1:7–21.

61. Tustison NJ, Cook PA, Klein A, Song G, Das SR, Duda JT, et al. Large-scale evaluation of ANTs and FreeSurfer cortical thickness measurements. Neuroimage [Internet]. 2014;99:166–79. Available from: http://dx.doi.org/10.1016/j.neuroimage.2014.05.044

62. Batalle D, Edwards AD, O'Muircheartaigh JO. Annual Research Review: Not just a small adult brain: understanding later neurodevelopment through imaging the neonatal brain. J Child Psychol Psychiatry. 2018;59(4):350–71.

63. Saygin ZM, Osher DE, Norton ES, Youssoufian DA, Beach SD, Feather J, et al. Connectivity precedes function in the development of the visual word form area. Nat Neurosci. 2016;19(9):1250–5.

64. Baron-Cohen S, Ring HA, Bullmore ET, Wheelwright S, Ashwin C, Williams SCR. The amygdala theory of autism. Neurosci Biobehav Rev [Internet]. 2000;24:355–64. Available from: papers2://publication/uuid/DA1D308F-7F1E-4C34-A17C-A86DBE70D978

65. Pine DS. Research Review : A neuroscience framework for pediatric anxiety disorders. J Child Psychol Psychiatry. 2007;48(7):631–48.

66. Warnell KR, Pecukonis M, Redcay E. Developmental relations between amygdala volume and anxiety traits: Effects of informant, sex, and age. Dev Psychopathol. 2018;30:1503–15.

67. Lonigan CJ, Phillips BM. Temperamental influences on the development of anxiety disorders. In: The developmental psychopathology of anxiety. New York, NY, US: Oxford University Press; 2001. p. 60–91.

Supporting information

S1 Fig. BaLa Overlap with dHCP DrawEm Amygdala Label in a representative neonate. (left) Coronal and axial slices depicting the basolateral amygdala (yellow) as defined by automated segmentation (Saygin et al., 2017), overlaid on the whole amygdala as defined by dHCP's DrawEm label (red). Overlap shown in orange (proportion overlap across all neonates: 0.76 ± 0.11)

S2 File. List of Anatomical Labels Combined to Create OTC.

S2 Fig. OTC label comparison in a representative individuals. (left) neonate, (right) adult. Dark blue = OTC 5 (anterior), blue = OTC 4, light blue = OTC 3, lime green = OTC 2, dark green = OTC 1 (posterior).

S1 Table. OTC Connectivity Differences Collapsed Across Samples. t-test results and corresponding p-values comparing mean connectivity between each OTC section, collapsed across adults and neonates.

S2 Table. OTC Connectivity Differences Within Each Sample. t-test results and corresponding p-values comparing mean connectivity between each OTC section, separately for adults and neonates.

S3 Table. OTC Connectivity Differences Between Samples. t-test results and corresponding p-values comparing mean-centered connectivity between adults vs. neonates in each OTC section, from 5 (anterior) to 1 (posterior). See Fig 1C in main manuscript.

S4 Table. Connectivity Differences Between Functional Parcels in Adults. t-test results and

corresponding p-values comparing mean connectivity between each functional parcel in adults.

S5 Table. Connectivity Differences Between Functional Categories in Adults. t-test results and corresponding p-values comparing mean connectivity between each functional category in adults.

S6 Table. Functional Category Connectivity Differences Between Samples. t-test results and corresponding p-values comparing mean-centered connectivity between adults vs. neonates for each functional category. See Fig 3B in main manuscript.

A)

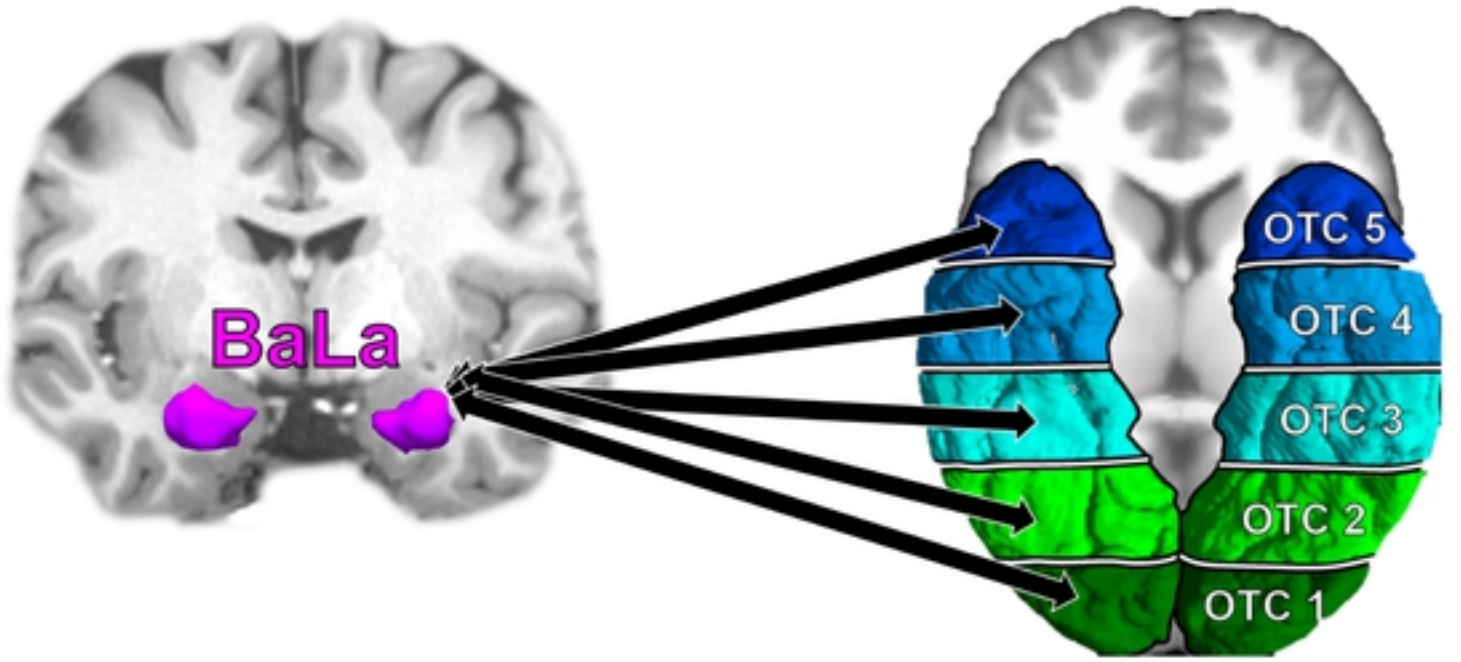
BaLa
OTC 5
OTC 4
OTC 3
OTC 2
OTC 1

B)

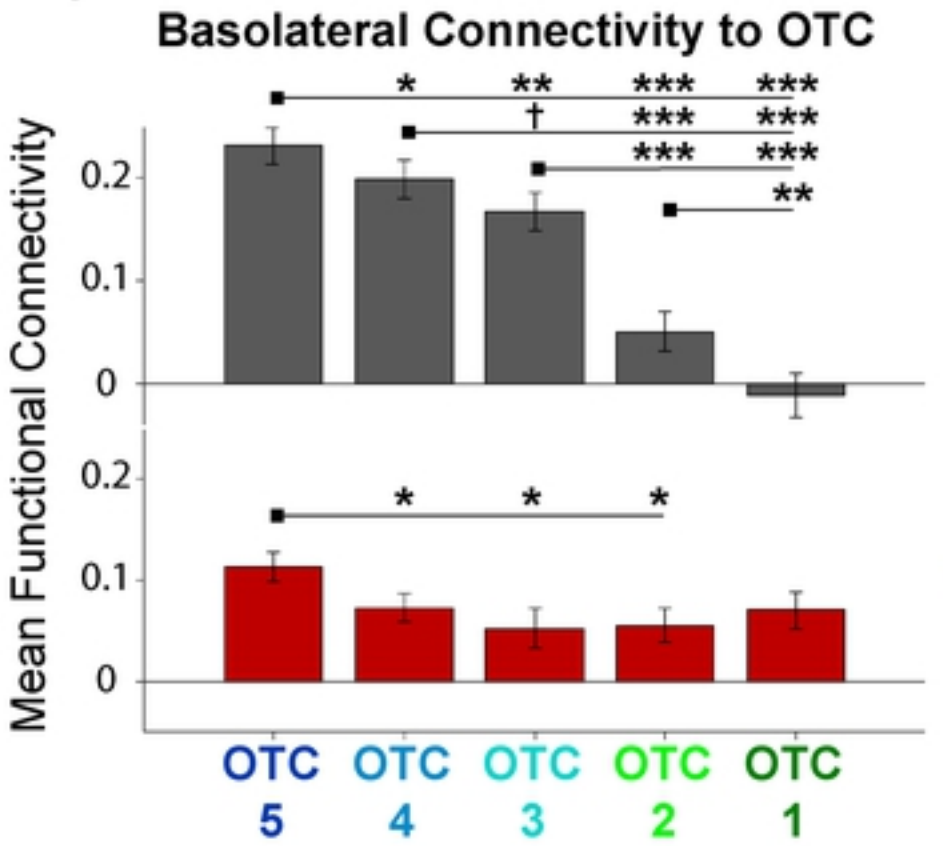
Basolateral Connectivity to OTC
Mean Functional Connectivity
0.2
0.1
0
OTC 5
OTC 4
OTC 3
OTC 2
OTC 1

C)

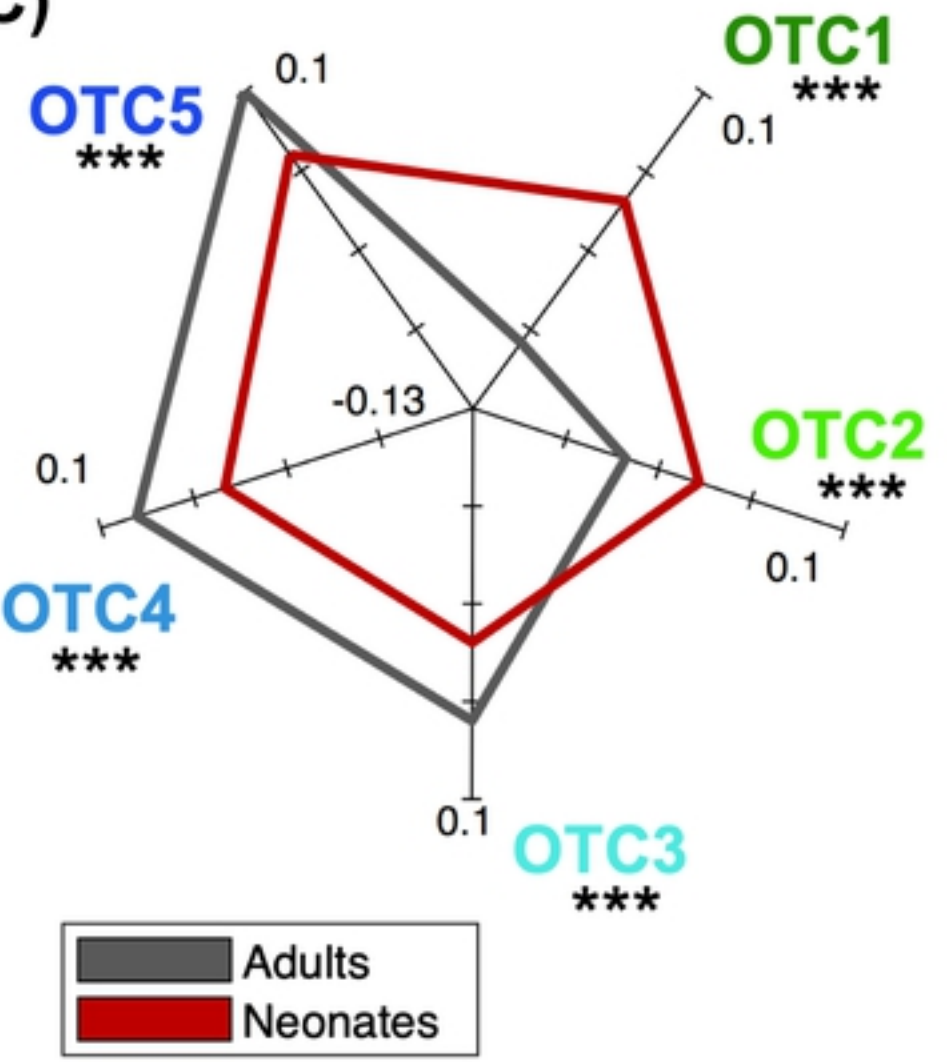
OTC5
***
OTC1
***
OTC2
***
OTC4
***
OTC3
***
0.1
-0.13
Adults
Neonates

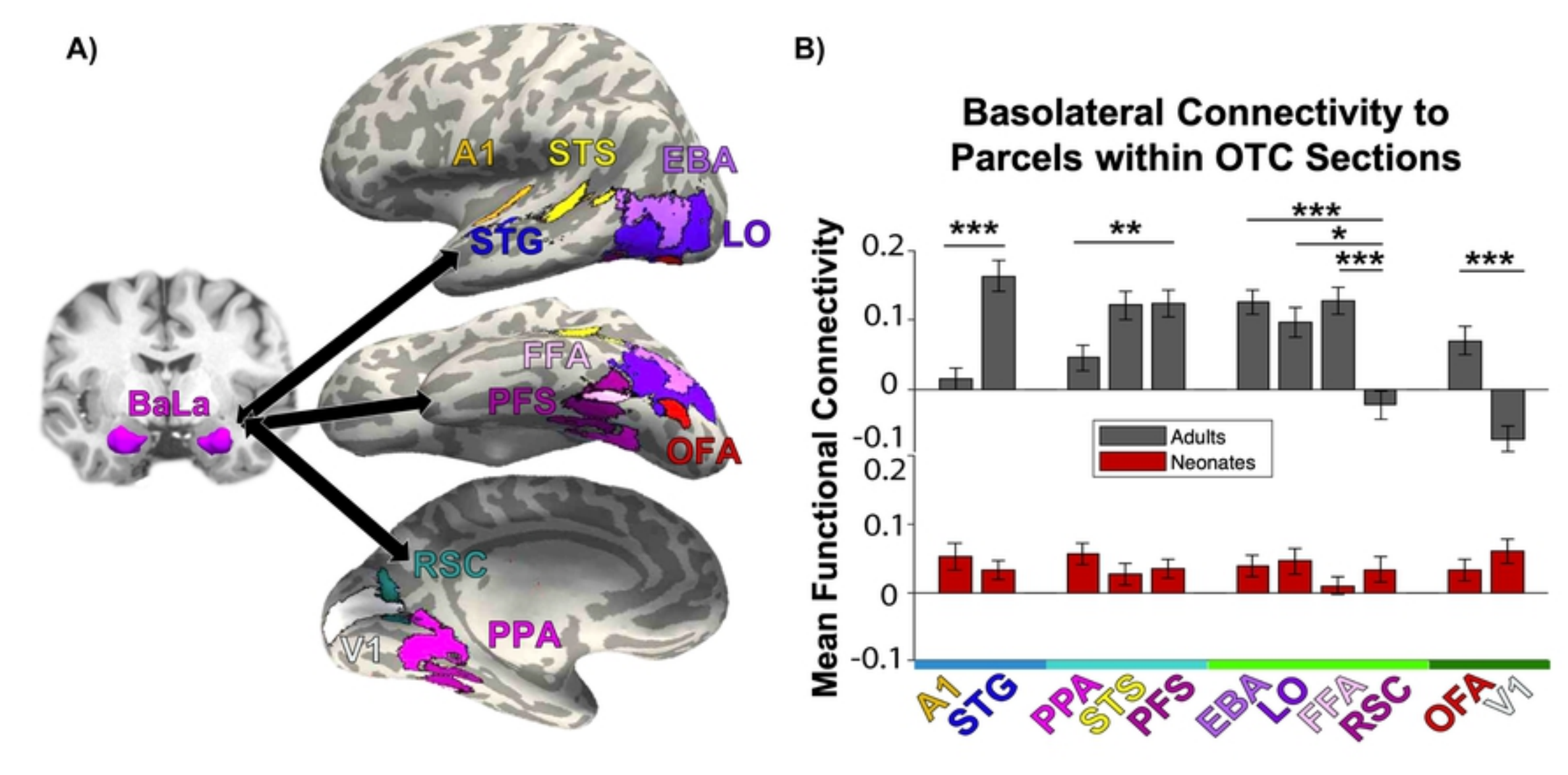
A)
A1
STS
EBA
STG
LO
BaLa
FFA
PFS
OFA
RSC
V1
PPA
B)
Basolateral Connectivity to
Parcels within OTC Sections
Mean Functional Connectivity
0.2
0.1
0
-0.1
***
**
***
*
***
***
Adults
Neonates
A1
STG
PPA
STS
PFS
EBA
LO
FFA
RSC
OFA
V1

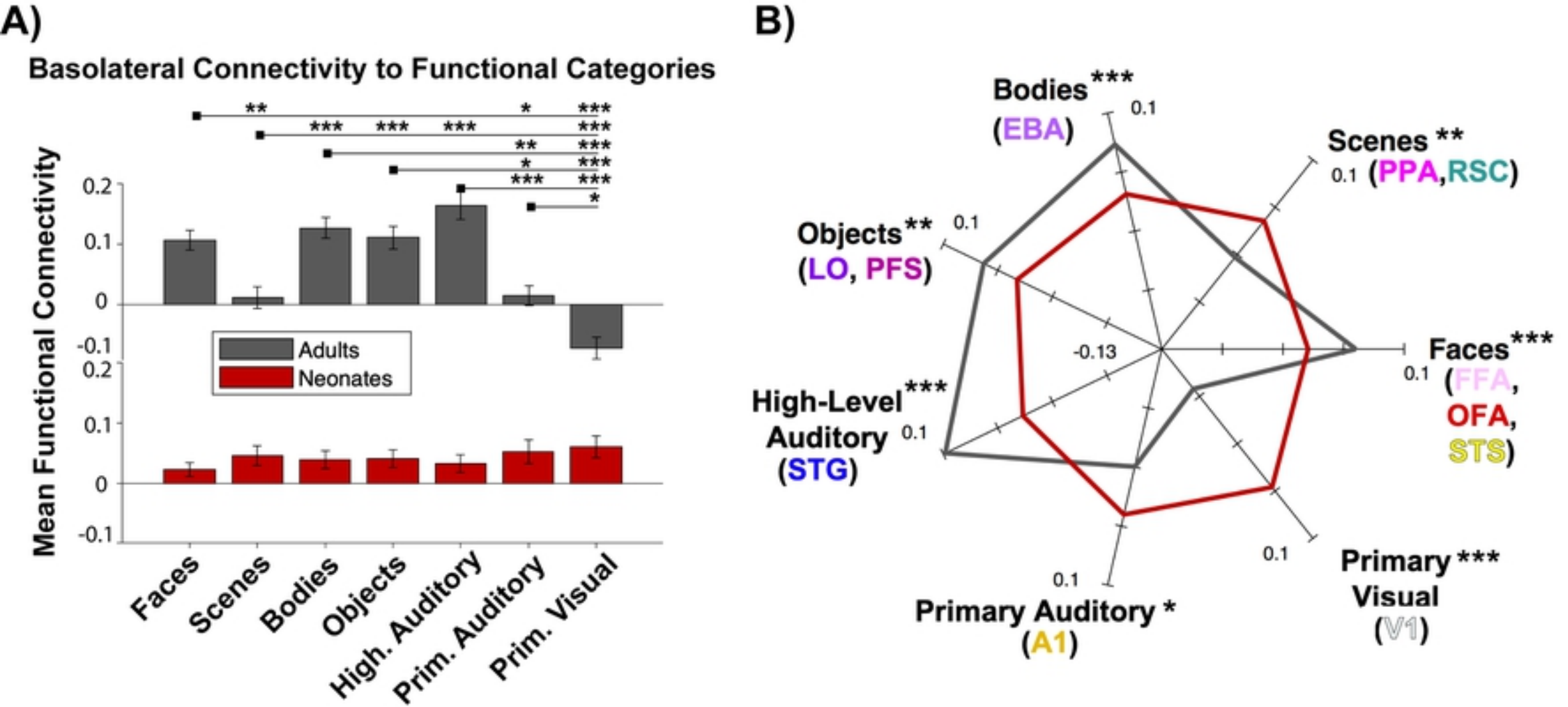
A)
Basolateral Connectivity to Functional Categories
Mean Functional Connectivity
0.2
0.1
0
-0.1
Adults
Neonates
Faces
Scenes
Bodies
Objects
High. Auditory
Prim. Auditory
Prim. Visual
B)
Bodies***
(EBA)
Scenes **
(PPA,RSC)
Objects**
(LO, PFS)
Faces***
(FFA,
OFA,
STS)
High-Level***
Auditory
(STG)
Primary***
Visual
(V1)
Primary Auditory *
(A1)
-0.13
0.1